2013

Magnetic properties and magnetocaloric effect of NdMn2−xTixSi2 compounds

M F. Md Din
University of Wollongong, mfmd999@uowmail.edu.au

Jianli Wang
University of Wollongong, jianli@uow.edu.au

S J. Campbell
University Of New South Wales, stewart.campbell@adfa.edu.au

R Zeng
University of Wollongong, rzeng@uow.edu.au

W D. Hutchison
University of New South Wales

See next page for additional authors

Publication Details

Md Din, M. F., Wang, J. L., Campbell, S. J., Zeng, R., Hutchison, W. D., Avdeev, M., Kennedy, S. J. & Dou, S. X. (2013). Magnetic properties and magnetocaloric effect of NdMn2-xTi xSi2 compounds. Journal of Physics D: Applied Physics, 46 (44), 1-11.

Magnetic properties and magnetocaloric effect of NdMn2–xTixSi2 compounds

Abstract

The structural and magnetic properties of the intermetallic compounds $NdMn_{2-x}Ti_xSi_2$ ($x = 0$, 0.1, 0.2, and 0.3) have been studied by x-ray and high resolution neutron powder diffraction, specific heat, dc magnetization, and differential scanning calorimetry measurements over the temperature range 3–450 K. The Curie temperature and Néel temperature of $NdMn_2Si_2$ decrease from $T_C = 36$ K and $T_N = 380$ K to $T_C = 14$ K and $T_N = 360$ K, respectively, on substitution of Ti ($x = 0.3$) for Mn. The magnetocaloric effect at the first order ferromagnetic phase transition at T_C, has been investigated in detail. Under a change of magnetic field of 0–5 T, the maximum value of the magnetic entropy change is 27 J kg^{-1} K^{-1} at $x = 0$, reducing to 15.3 J kg^{-1} K^{-1} at $x = 0.1$ and 10 J kg^{-1} K^{-1} at $x = 0.3$; importantly, no thermal or field hysteresis losses occur (eliminated from 0.3 K and 28.5 J kg^{-1} at $x = 0$ around T_C) with increase in Ti concentration. Combined with the lack of any hysteresis effects, these findings indicate that $NdMn_{1.9}Ti_{0.1}Si_2$ compound offers potential as a candidate for magnetic refrigerator applications in the temperature region below 35 K.

Keywords

ndmn2, effect, magnetocaloric, properties, magnetic, xsi2, compounds, xti

Disciplines

Engineering | Physical Sciences and Mathematics

Publication Details

Md Din, M. F., Wang, J. L., Campbell, S. J., Zeng, R., Hutchison, W. D., Avdeev, M., Kennedy, S. J. & Dou, S. X. (2013). Magnetic properties and magnetocaloric effect of NdMn2-xTi xSi2 compounds. Journal of Physics D: Applied Physics, 46 (44), 1-11.

Authors

M F. Md Din, Jianli Wang, S J. Campbell, R Zeng, W D. Hutchison, M Avdeev, S J. Kennedy, and S X. Dou

Magnetic Properties and Magnetocaloric Effect of $NdMn_{2-x}Ti_xSi_2$ Compounds

M. F. Md Din[1,4 *], J. L. Wang[1,2 +], S.J. Campbell[3], R. Zeng[1], W.D. Hutchison[3], M. Avdeev[2], S.J. Kennedy[2] and S. X. Dou[1]

[1]Institute for Superconductivity and Electronic Materials, University of Wollongong, Wollongong, NSW 2522, Australia
[2] Bragg Institute, Australian Nuclear Science and Technology Organization, Lucas Heights, NSW 2234, Australia
[3] School of Physical, Environmental and Mathematical Sciences, The University of New South Wales Canberra, The Australian Defence Force Academy, ACT 2600, Australia
[4]Department of Electrical & Electronic Engineering, Faculty of Engineering, National Defence University of Malaysia, Kem Sungai Besi, 57000 Kuala Lumpur, Malaysia

E-mail address: * mfmd999@uowmail.edu.au; + jianli@uow.edu.au

Fax: +61 2 4221 5731

Abstract

The structural and magnetic properties of the intermetallic compounds $NdMn_{2-x}Ti_xSi_2$ (x = 0, 0.1, 0.2, and 0.3) have been studied by X-ray and high resolution neutron powder diffraction, specific heat, dc magnetization, and differential scanning calorimetry measurements over the temperature range 3-450 K. The Curie temperature and Néel temperature of $NdMn_2Si_2$ decrease from T_C = 36 K and T_N = 380 K to T_C = 14 K and T_N = 360 K respectively on substitution of Ti (x = 0.3) for Mn. The magnetocaloric effect at the first order ferromagnetic phase transition at T_C, has been investigated in detail. Under a change of magnetic field of 0-5 T, the maximum value of the magnetic entropy change is 27 J kg^{-1} K^{-1} at x = 0, reducing to 15.3 J kg^{-1} K^{-1} at x = 0.1 and 10 J kg^{-1} K^{-1} at x = 0.3; importantly no thermal or field hysteresis losses occur (eliminated from 0.3 K and 28.5 J kg^{-1} at x=0 around T_C) with increase in Ti concentration. Combined with the lack of any hysteresis effects, these findings indicate that $NdMn_{1.9}Ti_{0.1}Si_2$ compound offers potential as a candidate for magnetic refrigerator applications in the temperature region below 35 K.

1. Introduction

Application of the magnetocaloric effect (MCE) for magnetic refrigeration offers advantages that are well known, with increasing prospects as the basis of magnetic cooling to replace conventional refrigeration systems over appropriate temperature regions [1-3]. Given these promising developments, magnetic materials which exhibit a large magnetocaloric effect have been studied, both experimentally and theoretically, over the past two decades [4, 5]. A number of materials which exhibit giant magnetic entropy changes at magnetic transitions have been investigated, including $Gd_5Si_2Ge_2$ [6], $(Mn, Fe)_2(P, Ge)$ [7], $MnAs_{1-x}Sb_x$ [8], and $La(Fe,Si)_{13}$ [9]. All of these materials undergo a first-order magnetic phase transition which, given the rapid change in magnetisation, enhances the scope for a large MCE. However such behaviour is often accompanied by hysteresis. For example, $La_{0.7}Pr_{0.3}Fe_{11.4}Si_{1.6}$ exhibits thermal hysteresis ~ 1.9 K and magnetic hysteresis ~ 0.2 T around T_C ~ 188 K [9]. The presence of a hysteresis effect in a material will lead to a decrease in efficiency of the energy performance during cooling and heating processes and therefore limit its use in practical applications. As such the search for suitable materials that show both a large MCE and are free from hysteresis continues.

The ternary intermetallic compounds of the RT_2X_2 series (R = rare earth, T = transition metal, X = Si or Ge) have attracted considerable attention because of the rich variety of interesting phenomena, including superconductivity, magnetism, mixed valence, heavy fermions, and Kondo behaviour [10, 11]. RT_2X_2 compounds form mainly in the $ThCr_2Si_2$ structure (space group $I4/mmm$), with the layered nature of this crystal structure leading to strong dependence of the magnetic interactions on the interplanar and intraplanar interatomic distances [12]. From this point of view, RMn_2X_2 compounds with X= Si or Ge have attracted special attention, due mainly to the interesting interplay between the magnetism of the layers of 3*d* and 4*f* atoms and the strong dependence of the magnitude of

the Mn moment and the magnetic state of the Mn sublattice on the Mn-Mn interatomic distances [11, 13-18].

As a general guide, for intraplanar distance, $d_{Mn\text{-}Mn}$ below ~ 2.87 Å, the coupling between Mn layers is antiferromagnetic while above this value, the coupling is ferromagnetic [19-21]. In $NdMn_2Si_2$, below T_N ~ 380 K the Mn sublattice orders antiferromagnetically, while below T_C ~ 36 K the compound is ferromagnetic with ordered moments at both the Nd and the Mn sublattices [22, 23]. These magnetic behaviours with different temperature dependences reflect different types of exchange interactions with different mechanisms with both the Ruderman-Kittel-Kasuya-Yosida (RKKY) exchange interaction *via* conduction electrons, and super exchange between magnetic atoms *via* the Si or Ge atoms contributing. Generally, the exchange interactions in RMn_2X_2 compounds can be divided into four classes: Mn–Mn within the Mn layers, Mn–Mn between the Mn layers, and Mn–R and R–R interactions [24].

Here, we present a detailed investigation of the influence of replacing Mn atoms by Ti atoms on the magnetic structure and magnetic phase transition in $NdMn_{2-x}Ti_xSi_2$ compounds. The main interest is to explore the effects of replacing Mn atoms of atomic radius r(Mn) = 1.35 Å and electronic configuration Mn ($3d^5 4s^2$) with larger Ti atoms of atomic radius r(Ti) = 1.45 Å and electron configuration Ti ($3d^2 4s^2$). In the case of $NdMn_{2-x}Co_xSi_2$ [25] for example, replacement of Mn by the smaller Co atoms, r(Co) = 1.25 Å of electronic configuration Co ($3d^7 4s^2$), leads to a decrease in magnetic entropy change from ~ 14.4 J kg^{-1} K^{-1} with x=0.2 to 12.4 J kg^{-1} K^{-1} with x=0.4 (ΔB = 0- 5 T) but the Curie temperature T_C ~ 45 K does not change with increasing Co concentration for $NdMn_{2-x}Co_xSi_2$ (x=0.2, 0.4, 0.8 and 1). In this study, we will investigate the effects of Ti substitution for Mn in $NdMn_2Si_2$ compound on the structural and magnetic properties. Given that Ti atoms (r(Ti) = 1.45 Å) are significantly larger than Mn atoms (r(Mn) = 1.35 Å) , replacement of Mn by Ti in $NdMn_2Si_2$

is expected to increase the distance between magnetic atoms, thus modifying the magnetic states of both the Nd and the Mn sublattices.

2. Experimental details

Polycrystalline samples with nominal compositions $NdMn_{2-x}Ti_xSi_2$ (x = 0, 0.1, 0.2, 0.3) were prepared by the arc melting of appropriate amounts of high purity constituent elements under a high purity argon atmosphere in a water-cooled copper crucible. The starting materials were pure elements (≥ 99.9%), and an excess of 3 at. % Mn was used to compensate for the loss during the arc melting and annealing processes. The ingots were turned over and re-melted several times to ensure homogeneity. The resulting ingots were wrapped in Ta foil and sealed under vacuum in a quartz tube, annealed at 900°C for 7 days to improve crystallization of the samples [26], and then quenched into water. The crystal structure of the samples were checked by room temperature powder X-ray diffraction (XRD) measurements using $CuK_{\alpha 1}$ radiation with the diffraction patterns refined using the Fullprof software package [27]. The magnetic properties were investigated over the temperature 10-300 K using the vibrating sample magnetometer option of a Quantum Design 14 T physical properties measurement system (PPMS) and an MPMS XL magnetic properties measurement system. Differential scanning calorimetry (DSC) measurements were carried out using a TA instrument DSC-Q100 over the range 300-450 K to check for possible phase transitions in the higher temperature range and investigate thermal hysteresis changes at the magnetic transitions. The crystallographic and magnetic structural behaviors of the set of $NdMn_{1.9}Ti_{0.1}Si_2$ samples were investigated over the temperature range 3-450 K by powder neutron diffraction experiments using the high resolution powder diffractometer Echidna (wavelength λ = 1.622(1) Å) at the Open Pool Australian Light Water Reactor (OPAL), Lucas Heights, Australia.

3. Results and Discussion

3.1. Crystal structure

Confirmation that all of the $NdMn_{2-x}Ti_xSi_2$ (x = 0, 0.1, 0.2, 0.3) samples crystallize in the expected $ThCr_2Si_2$ type structure with space group I4/mmm [28] was provided by analysis of the X-ray powder diffraction patterns. $NdMn_{2-x}Ti_xSi_2$ compounds have Nd atoms in the 2a site (0, 0, 0), while Ti and Mn share the position at the 4d site (0, $\frac{1}{2}$, $\frac{1}{4}$), and Si atoms occupy the 4e site (0, 0, z). The measured data from the diffraction patterns were analysed using the Rietveld refinement technique [27], and the distances between neighbouring atoms (Tables 1 and 3) have been obtained with the BLOKJE program [29], using the structural and positional parameters. Compared with pure $NdMn_2Si_2$ [22, 28], substitution of Ti for Mn does not change the crystal structure but leads to an expansion of the unit cell. The lattice constants *a* and *c*, and correspondingly the unit cell volumes, were found to increase with the Ti content consistent with the larger atomic radius of Ti compared to Mn. As shown in Table 1, $d_{\text{Mn-Mn}}$ increases from 2.8312(6) Å for x=0 to 2.8341(6) Å for x=0.3. However $d_{\text{Mn-Mn}}$ remains below $d_{\text{Mn-Mn}}^{\text{crit}}$ = 2.87 Å for all compositions. The geometric influence due to the size difference of Ti and Mn can be understood in the term of chemical pressure using the Murnaghan equation of state (see e.g. the case of $PrMn_{2-x}Fe_xGe_2$ compounds [26]):

$$p = \left(\frac{B_0}{B'_0}\right)\left[\left(\frac{V}{V_0}\right)^{-B_0} - 1\right] \quad (1)$$

where B_0 is the isothermal bulk modulus, B'_0 is its pressure derivative , and V_0 and V are the volume at ambient pressure and pressure *p*, respectively. Using the values of B_0 = 867 kbar, B'_0 = 5.1 for $CeNi_2Ge_2$ [30], the corresponding pressure can derived to be -3.35 kbar, -5.35 kbar and -6.05 kbar for the $NdMn_{2-x}Ti_xSi_2$ samples (x=0.1, 0.2 and 0.3) respectively. As discussed below these changes in $d_{\text{Mn-Mn}}$ distances influence the magnetic properties.

3.2. Magnetic studies

The temperature dependence of the magnetization of $NdMn_{2-x}Ti_xSi_2$ (x = 0, 0.1, 0.2, 0.3) measured in a magnetic field of B = 0.01 T over the temperature range ~ 10-300 K is shown in figure 1 together with the differential scanning calorimetry (DSC) curves over the temperature range ~ 300-450 K. The inset shows the values of the Néel temperature T_N and the Curie temperature T_C, for the set of compounds as defined by 1/M versus temperature and the maxima of the dM/dT versus temperature graphs respectively. For the DSC measurements, the phase transition temperatures were determined by the maxima of the DSC signals (see figure 1). Comparison of results obtained under otherwise identical conditions for cooling and warming revealed almost no thermal hysteresis across all compositions (ΔT = 0.3 K at x=0 and ΔT = 0 K at x = 0.1, 0.2 and 0.3). Inspection of the insert to figure 1, reveals that T_N decreases from ~ 380 K to ~ 360 K with increase in Ti concentration from x = 0 to x = 0.3 while T_C decreases from ~ 36 K to ~ 14 K.. As shown in Table 1 $d_{Mn\text{-}Mn}$ and $d_{Mn\text{-}Nd}$ are found to increase from $d_{Mn\text{-}Mn}$ = 2.8312(6) Å, $d_{Mn\text{-}Nd}$ = 3.3063(6) Å at x = 0 to $d_{Mn\text{-}Mn}$ = 2.8341(6) Å, $d_{Mn\text{-}Nd}$ = 3.3180(6) Å at x = 0.3 and this expansion (size effect) will lead to enhancement of the Mn-Mn intralayer exchange interaction. On the other hand, increased Ti concentration is also expected to weaken the exchange interactions of Mn-Mn between layers and the Mn-Nd due to the magnetic dilution effect. Moreover, the change in electronic environment on replacing Mn ($3d^5 4s^2$) by Ti ($3d^2 4s^2$) is also expected to influence the magnetic structures and states of the $NdMn_{2-x}Ti_xSi_2$ compounds. This is supported by Density Functional Theory calculations for RMn_2Ge_2 (R = Y or Ca) compounds [31] which indicate that to a large extent, the magnetic moment is determined mainly by the interatomic Mn-Mn distances, while the interstitial electron density contributes to the change in magnetic structures. Assuming the expansion of the unit cell volume due to Ti substitution (chemical pressure) to be equivalent to the influence of external pressure [26] and using dT_C/dp = -0.6

K/kbar in $NdMn_2Ge_2$ [32] (the same crystal structures), as a guide for the modulus values for $NdMn_{2-x}Ti_xSi_2$, the magnetic transition temperatures, T_C, expected from the pressure effect due to replacement of Mn atoms by the larger Ti atoms have been calculated as shown in figure 2. The analysis based on the Murnaghan relationship indicates a slight increase in T_C with Ti concentration from T_C = 36 K for x = 0 to T_C = 37 K for x = 1 whereas the experimental data reveal a decrease from T_C = 36 K for x = 0 to T_C = 14 K for x = 0.3. These results indicate that for $NdMn_{2-x}Ti_xSi_2$ compounds over the Ti concentration range x = 0.0 to 1.0, the electronic effects, rather than atomic size effects produce the observed decrease in magnetic transition temperature (T_C; Fig 2).

The magnetization versus field curves (B = 0-5 T) for $NdMn_{2-x}Ti_xSi_2$ (x = 0, 0.1, 0.2, 0.3) at 10 K are shown in figure 3. The magnetization is not saturated up to 5 T indicating large magnetic anisotropy in these samples. This behaviour is supported by the strong uniaxial magnetic anisotropy observed for $NdMn_2Si_2$ [22] with the moment of 4.16 μ_B/f.u. inhibiting saturation in magnetization up to fields of B = 5 T. The saturation magnetization values at 10 K were derived from graphs of magnetisation M versus 1/B by extrapolation and applying the law of approach to saturation. The saturation magnetization, M_S (at 10 K) is found to decrease with increasing Ti concentration in the $NdMn_{2-x}Ti_xSi_2$ compounds (Table 2). If we assume that the rare earth moment does not change with Ti content, it can be derived that the substitution of Ti atoms for Mn leads to a decrease of around -4.6 μ_B per Ti atom (from linear fitting), which is much faster than that expected with a simple dilution model (in which the Ti atoms do not carry magnetic moment). This behaviour is similar to that observed in $NdMn_{2-x}Co_xSi_2$ (-2.1 μ_B per Co atom decrease of M_s at 5 K) [25], $NdMn_{2-x}Cr_xSi_2$ (-2.8 μ_B per Cr atom decrease of M_s at 4.2 K) [33] and $NdMn_{2-x}Fe_xSi_2$ [34] compounds.

The magnetization curves obtained for $NdMn_2Si_2$ and $NdMn_{1.9}Ti_{0.1}Si$ for fields in the range B = 0 - 8 T and B = 0 - 5 T around their ferromagnetic ordering temperatures are

shown in figures 4(a) and 4(b), respectively. These data were obtained for increasing and decreasing fields at 2 K intervals spanning a range of about 45 K around T_C, thus providing information about magnetic hysteresis loss effects as discussed below using expression [35]:

$$\text{Magnetic hysteresis loss} = \int_{decrease\ H}^{increase\ H} (\partial M)_H \ dH. \quad (2)$$

Magnetic hysteresis effects (as indicated by the area enclosed between the ascending and descending branches of the magnetization curves) are also characteristic of first order magnetic transitions. As demonstrated in figure 4(c), comparison of the magnetisation curves around the ferromagnetic ordering temperatures for $NdMn_2Si_2$ (figure 4(a)) with those for $NdMn_{1.9}Ti_{0.1}Si_2$ (figure 4(b)) reveal pronounced hysteresis losses of up to ~ 28.5 J kg^{-1} (indicated values for B = 0 - 5 T as suitable to comparison) for $NdMn_2Si_2$ at T_C = 36 K while negligible hysteresis losses of ~ 0.8 J kg^{-1} are observed for $NdMn_{1.9}Ti_{0.1}Si_2$ around T_C = 22 K. It is demonstrated clearly in figure 4(c) that magnetic hysteresis losses decrease significantly on substitution of Ti for Mn. This behaviour indicates that increasing Ti concentration contributes to a weakening of the characteristic field induced metamagnetic transition from the antiferromagnetic to the ferromagnetic state. As shown in figure 5(a) for $NdMn_2Si_2$, with the applied field below the critical value field (H_C), the magnetization increases linearly with increasing field applied expected for an antiferromagnetic state. However for applied field greater than H_C, the magnetization initially increases rapidly before tending towards saturation at higher fields (similar behaviour is observed for $La_{0.5}Pr_{0.5}Mn_2Si_2$ [11] of the same $ThCr_2Si_2$ bct crystal structure) i.e. ferromagnetic behaviour. In the present investigation, as shown in figure 5(b) the value of H_C is found to increase significantly with increasing the temperature and Ti concentration. Welter *et al* [22] have postulated that the ferromagnetic ordering of Nd sublattice below T_C drives the change in order of the Mn sublattice from antiferromagnetism to ferromagnetism in $NdMn_2Si_2$. It can be seen from figures 4(a) and 4(b) that the metamagnetic transition occurs at higher temperatures and lower values of H_C in

$NdMn_2Si_2$ compared with $NdMn_{0.9}Ti_{0.1}Si_2$. Therefore the metamagnetic transition is expected to produce a larger magnetocaloric effect for x = 0, with a decrease in MCE values for x = 0.1, 0.2 and 0.3 as described below in the magnetic entropy section.

As mentioned before, significant MCE values and magnetic entropy changes are usually obtained with a first order magnetic transition due to a large rate of change of magnetisation. Although such materials have this advantage compared with materials that exhibit a second order transition, first order magnetic transitions usually exhibit considerable thermal hysteresis and magnetic hysteresis. Here we have established that hysteresis effect have effectively been eliminated by substitution of Mn with Ti in $NdMn_{2-x}Ti_xSi_2$ compounds. Figures 6(a - d) show the corresponding Arrott plots (M^2 versus B/M) for the x = 0, 0.1, 0.2 and 0.3 samples, respectively. The Arrott plots are found to exhibit features characteristic of a first order transition for all of the samples. In particular the S-shaped nature of the Arrott plot near T_C denotes a negative order of the sign of the coefficient c2(T) in the Landau expansion of the magnetic free energy [36], thereby denoting a first order magnetic transition. The present findings demonstrate that the ferromagnetic transition at T_C in $NdMn_{2-x}Ti_xSi_2$ remains a first order transition on substitution of Ti for Mn to Ti concentration up to x=0.3.

3.3. Magnetic entropy; magnetocaloric effect

The magnetic entropy change, $-\Delta S_M$, has been determined for the set of $NdMn_{2-x}Ti_xSi_2$ compounds (x = 0, 0.1, 0.2 and 0.3) from their magnetization curves for both increasing and decreasing field values as functions of temperature and magnetic field (ΔB = 0-5 T). The magnetic entropy change has been derived by applying the standard Maxwell relation [37]:

$$-\Delta S_M(T,H) = \int_0^H \left(\frac{\partial M}{\partial T}\right)_H dH. \quad (3)$$

As shown by the curves of figure 7(a), the $-\Delta S_M$ peak (closed symbols for increasing field values and open symbols for decreasing field values) gradually broadens towards higher

temperatures with increasing magnetic field (from ΔB = 0-5 T), behaviour characteristic of a field induced transition from an antiferromagnetic to a ferromagnetic state.

The changes in magnetic entropy for the set of $NdMn_{2-x}Ti_xSi_2$ compounds (x = 0, 0.1, 0.2 and 0.3) around their ferromagnetic ordering temperatures are shown in figure 7(b) as calculated from decreasing applied fields in order to satisfy the suitability of different experimental and related analytical approaches to establish the isothermal entropy change [38]. The entropy values at the respective Curie temperatures are (ΔB = 0-5 T): $-\Delta S_M$ ~ 27 J kg^{-1} K^{-1} at T_C = 36 K; $-\Delta S_M$ ~ 15.3 J kg^{-1} K^{-1} at T_C = 22 K; $-\Delta S_M$ ~ 13 J kg^{-1} K^{-1} at T_C = 16 K and $-\Delta S_M$ ~ 10 J kg^{-1} K^{-1} at T_C = 14 K. The decrease in magnetization on substitution of the non-magnetic Ti for Mn, correspondingly reduces the value of $-\Delta S_M$. Never the less it is noted that the MCE values of $-\Delta S_M$ ~ 15.3 J kg^{-1} K^{-1} for $NdMn_{1.9}Ti_{0.1}Si_2$ and $-\Delta S_M$ ~ 13 J kg^{-1} K^{-1} for $NdMn_{1.8}Ti_{0.2}Si_2$ are comparable with MCE values for other materials with small hysteresis that exhibit transitions in the temperature region below 100 K. These materials include: $TbCoC_2$ [39] ($-\Delta S_M$ = 15 J kg^{-1} K^{-1} at 28 K), GdCoAl [40] ($-\Delta S_M$ = 10.4 J kg^{-1} K^{-1} at 100 K) and TbCoAl [40] ($-\Delta S_M$ = 10.5 J kg^{-1} K^{-1} at 70 K), all of which - in common with $NdMn_{1.9}Ti_{0.1}Si_2$ and $NdMn_{1.8}Ti_{0.2}Si_2$ - importantly exhibit no field hysteresis losses.

The magnetic entropy change, $-\Delta S_M$ (*T, B*) has also been derived from heat calorimetric measurements of the field dependence of the heat capacity using the expression [2, 41, 42]:

$$-\Delta S_M(T,B) = \int_0^T \left(\frac{C(T,B)-C(T,0)}{T}\right) dT \quad (4)$$

where *C(T,B)* and *C(T,0)* are the values of the heat capacity measured in field *B* and zero field, respectively. The corresponding adiabatic temperature change, ΔT_{ad} can be evaluated from $-\Delta S_M$ (*T, B*) and the zero field heat capacity data as:

$$\Delta T_{ad}(T,B) = \int_0^B \frac{T}{C_{B,P}} \left(\frac{\partial M}{\partial T}\right)_B dB \quad (5)$$

Figure 8(b) shows the set of heat capacity measurement obtained for $NdMn_{1.9}Ti_{0.1}Si_2$ with B = 0, 2, and 5 T. The corresponding $-\Delta S_M(T, B)$ values for $NdMn_{1.9}Ti_{0.1}Si_2$ are shown in figure 8(a) with the ΔT_{ad} values shown in figure 8(c). The peak value of the adiabatic temperature change is ΔT_{ad}^{max} = 4.7 K for ΔB = 0-5 T. As shown in figure 8(a), the maximum magnetic entropy change for $NdMn_{1.9}Ti_{0.1}Si_2$ as determined from the heat capacity measurements of $-\Delta S_M^{max}$ ~ 15 J kg^{-1} K^{-1} and 9.3 J kg^{-1} K^{-1} for ΔB = 0-5 T and 0-2 T are similar to the maximum entropy change $-\Delta S_M^{max}$ ~ 15.3 J kg^{-1} K^{-1} and 9.8 J kg^{-1} K^{-1} as determined from the magnetic measurements using the Maxwell relation. The good agreement between the two sets of measurements confirms that the $-\Delta S_M$ values derived for $NdMn_{1.9}Ti_{0.1}Si_2$ from the magnetization measurements represent the MCE behaviour within experimental errors [6, 17, 43]. By comparison, Nikitin *et al* [44] reported that the value of ΔT_{ad}^{max} in $NdMn_2Si_2$ compound (around T_C ~ 32 K) can be up to 8.2 K with a field change of ΔB=0-6 T.

In general, the relative cooling power (RCP) is an important parameter of the magnetocaloric material, providing an accepted criterion to evaluate the refrigeration efficiency in practical application. The RCP is used to evaluate the cooling power of magnetic refrigerants by measuring how much heat can be transferred between two temperatures (low and high in temperature span range) in one ideal refrigeration cycle. The RCP is defined by the following expression [45]:

$$\mathrm{RCP} = -\Delta S_M^{\max} \delta T^{\mathrm{FWHM}}. \quad (6)$$

$-\Delta S_M^{\max}$ denotes the maximum entropy change and δT represents the full width at half maximum (FWHM) of the temperature dependence of the magnetic entropy change $-\Delta S_M$. A summary of the RCP values and other magnetic characterization parameters for $NdMn_{2-x}Ti_xSi_2$ (x = 0, 0.1, 0.2, 0.3) compounds is listed in Table 2. The RCP shows the same trend with Ti concentration as the magnetic entropy change. It is noted that δT increases with Ti content: δT = 9.5 K, δT = 12.0 K, δT = 12.4 K and δT = 12.8 K for x=0, 0.1, 0.2 and 0.3

respectively. It was found that the RCP decreases from ~127 J kg^{-1} for x = 0 to ~70 J kg^{-1} for x = 0.3 for a change in magnetic field ΔB = 0-5 T.

3.4. Magnetic Structures of $NdMn_{1.9}Ti_{0.1}Si_2$ - Neutron diffraction

The $NdMn_{1.9}Ti_{0.1}Si_2$ compound was selected for investigation by neutron diffraction measurements over the temperature range 3-450 K as representative of the magnetic behaviour of the $NdMn_{2-x}Ti_xSi_2$ samples (figure 1). The aims were to determine the magnetic structures and to explore structural changes at the transition temperatures. The diffraction patterns (λ = 1.622(1) Å) and Rietveld refinements obtained for $NdMn_{1.9}Ti_{0.1}Si_2$ at 450 K, 150 K and 15 K are shown in figures 9(a), 9(b) and 9(c), respectively. The selected temperatures typify the behaviour of $NdMn_{1.9}Ti_{0.1}Si_2$ in the three magnetic regions (paramagnetic-antiferromagnetic-ferromagnetic) as indicated from the magnetisation and DSC measurements of figure 1. Rietveld refinements of the neutron diffraction pattern at 450 K (figure 9(a)) confirm that $NdMn_{1.9}Ti_{0.1}Si_2$ has the $ThCr_2Si_2$ structure as expected. The absence of magnetic scattering above T_N ~ 374 K (figure 1) in reflections such as (101), (111) and (112) is consistent with a paramagnetic (PM) state. (*cf.* e.g. the disordered magnetic states (PM) observed in $PrMn_{1.6}Fe_{0.4}Si_2$ [26], $EuMn_2Si_2$ [46] and $LaPrMn_2Si_2$ [47]). Below T_N ~ 374 K, $NdMn_{1.9}Ti_{0.1}Si_2$ is found to exhibit the antiferromagnetic interlayer coupling structure (AFil) down to T_C ~ 22 K (see e.g. the 150 K pattern of figure 9(b)). The AFil structure – a collinear antiferromagnetic structure between adjacent Mn planes in a + - + - sequence along the *c*-axis – is indicated by the magnetic scattering observed at the (111), (113) and (201) reflections; (extinction rules $h + k = 2n$ and $h + k + l = 2n+1$) in agreement with Dincer *et al* [47]. In order to draw out the changes in magnetic structures with temperature, the temperature dependence of the peak intensity for selected magnetic peaks is shown in figure 9(d). Furthermore, the absence of magnetic scattering from the (111), (113)

and (201) reflections at 15 K in figure 9(c), combined with the increase in intensity of the (112) and (101) peaks as in figure 9(d), indicate that the interlayer spin components of the Mn moments align parallel, thus leading to a canted ferromagnetic structure (Fmc) for the Mn sublattice. The presence of the purely magnetic peak (001) below T_C indicates the existence of antiferromagnetic component of Mn moment in the ab-plane [22]. At lower temperature (e.g. 3 K; figure 9(d)), the increase in the intensities of the (112) (contributions from both Nd- and Mn-sublattices) and (101) (contribution only from Nd-sublattice [22]) reflections further indicates an additional contribution from Nd moments coupled parallel to the Mn moments along *c*-axis thereby leading to the formation of Fmc+F(Nd) magnetic structure as depicted in figures 9(e). This behavior agrees well with the results of Welter *et al* [48] who demonstrated that in the RMn_2Ge_2 compounds with R= Pr and Nd rare earth moments ferromagnetically coupled with the Mn sublattice at low temperatures. This behaviour, also applicable to $NdMn_2Si_2$ [22] and $NdMn_2Si_{1.6}Ge_{0.4}$ [17] compounds, is due to the exchange interaction between the light rare earth elements and 3*d* transition metal as reported by Coey [49]. Ordering of the Nd sublattice in $NdMn_2Si_2$ below T_C has also been confirmed by Chatterji *et al* [50] from inelastic neutron scattering.

The variation in the *a* and *c* lattice parameters with temperature are plotted in figure 10(a). Both the *a* and *c* values exhibit a monotonic decrease with temperature in the region of the antiferromagnetic transition between T_N = 374 K and T_C = 22 K, while below T_C = 22 K, the *a* lattice parameter expands slightly from 3.998 Å at 35 K to 4.001 Å at 3 K whereas the *c* lattice parameter decreases from 10.536 Å at 35 K to 10.523 Å at 3 K. The variation in lattice parameters *a* and *c* shown in figure 10(a) for the PM, AFil, and Fmc+F(Nd) states is comparable with the behaviour in $NdMn_2Si_2$ [22]. The changes in lattice parameter at $T_C \sim 22$ K when the magnetic state changes from AFil to Fmc+F(Nd) structure, indicates the presence of strong magnetostructural coupling around T_C. As discussed recently [51, 52], the strong

magnetostructural coupling leads to a large structural entropy change around the magnetic phase transition, thereby contributing to the total entropy change around T_C.

Figure 10(b) is a plot of the temperature dependence of the Mn magnetic moments as derived from the refinements. Within the AFil state region (T_N ~ 374 K > T > T_C ~ 22 K), the Mn moment increases to μ^{Mn} = 2.1 (1) μ_B at 50 K with both Nd and Mn ordering magnetically below T_C ~ 22 K. The magnetic moments for Mn and Nd have been derived to be μ_{total}^{Mn} = 1.56 (4) μ_B (of basal plane and axial components μ_{ab}^{Mn} =0.86(2) μ_B and μ_c^{Mn} =1.30(6) μ_B respectively) and μ^{Nd} = 2.56(5) μ_B at 3 K. The Nd moment and the ferromagnetic component of the Mn moment along the *c*-axis for $NdMn_{1.9}Ti_{0.1}Si_2$ are found to be 2.56(1) μ_B and 1.30(1) μ_B respectively. The resultant total moment is 3.86(1) μ_B per formula unit at 3 K which is slightly higher than that obtained from DC magnetization measurement at 10 K (3.6 μ_B per formula unit). We suggest this different value of magnetic moment is related to the non-saturation behavior shown by the magnetisation curve from DC measurements at 10 K even for a field applied of 5 T.

4. Conclusions

A systematic investigation of the structural and magnetic characteristics of $NdMn_{2-x}Ti_xSi_2$ (x = 0, 0.1, 0.2 and 0.3) compounds has been carried out. Substitution of Ti for Mn leads to decreases in the Curie temperature and the Néel temperature from T_C ~ 36 K and T_N ~ 380 K at x=0 to T_C ~ 14 K and T_N ~ 360 K at x=0.3. The variation in the value of T_C with increasing Ti concentration can be understood in terms of changes in the Mn-Mn exchange interaction together with the effects of magnetic dilution and chemical pressure. A metamagnetic transition from the antiferromagnetic to the ferromagnetic state due to the application of magnetic field was observed above T_C for $NdMn_{1.9}Ti_{0.1}Si_2$. Substitution of Mn by Ti leads to a reduction of the magnetic entropy change from $-\Delta S_M$ ~ 27 J kg^{-1} K^{-1} at x = 0; $-\Delta S_M$ ~ 15.3 J kg^{-1} K^{-1} at x = 0.1; $-\Delta S_M$ ~ 13 J kg^{-1} K^{-1} at x=0.2 and $-\Delta S_M$ ~ 10 J kg^{-1} K^{-1} at x = 0.3

respectively. However, analysis of the magnetisation data demonstrates that the first order magnetic transition of $NdMn_2Si_2$ around T_C remains unchanged on replacement of Mn by Ti, and this substitution leads to significant reduction in magnetic hysteresis losses from 28.5 J kg^{-1} for $NdMn_2Si_2$ to 0.8 J kg^{-1} for $NdMn_{1.9}Ti_{0.1}Si_2$ with ΔB = 0-5 T and eliminates thermal hysteresis from ΔT = 0.3 K at x = 0 to ΔT = 0 K at x = 0.1. Neutron diffraction studies demonstrate that $NdMn_{1.9}Ti_{0.1}Si_2$ has the AFil antiferromagnetic structure in the temperature range T_N ~ 374 K > T > T_C ~ 22 K and the combined Fmc+F(Nd) ferromagnetic state below T_C ~ 22 K. Ti substitution in $NdMn_{2-x}Ti_xSi_2$ compounds result in material with useful magnetocaloric effect behaviour and free of magnetic and thermal hysteresis loss.

Acknowledgments

This work was supported in part by a grant from the Australian Research Council Discovery Projects (DP0879070; DP110102386). M.F.M.D. acknowledges the Ministry of Higher Education, Malaysia for a postgraduate research scholarship.

Tables

Table 1. Lattice parameters, unit cell volume, and Mn-Mn distance of the $NdMn_{2-x}Ti_xSi_2$ compounds with x = 0, 0.1, 0.2 and 0.3 as determined from refinement of the room temperature X-ray diffraction patterns. The errors are shown for $NdMn_2Si_2$ as a typical example.

$NdMn_{2-x}Ti_xSi_2$	a (Å)	c (Å)	V (Å^3)	c/a	d_{Mn-Mn} (Å)	d_{Mn-Nd} (Å)
x=0	4.0039(5)	10.5251(6)	168.73(4)	2.6287(3)	2.8312(6)	3.3063(6)
x=0.1	4.0067	10.5515	169.39	2.6335	2.8332	3.3124
x=0.2	4.0073	10.5743	169.81	2.6388	2.8336	3.3171
x=0.3	4.008	10.5779	169.92	2.6392	2.8341	3.318

Table 2. Results of the magnetic characterization of $NdMn_{2-x}Ti_xSi_2$ compounds with x = 0, 0.1, 0.2 and 0.3. The magnetic features listed are: Curie temperature (T_C; determined by graphs of dM/dT versus T) and the order of the magnetic transition around T_C; Néel temperature (T_N; determined by graphs of 1/M versus T) and the saturation magnetization, M_S, as determined at 10 K. The magnetic entropy change ($-\Delta S_M$) and the relative cooling power (RCP) are given for a field change of 0-5 T. The errors are shown for $NdMn_2Si_2$ as a typical example.

Composition	T_C (K)	Nature of Transition at T_C	T_N (K)	M_S (μ_B/f.u.) (T=10 K)	$-\Delta S_M$ (J kg^{-1} K^{-1}) (B=0-5 T)	RCP (J kg^{-1}) (B=0-5 T)
$NdMn_2Si_2$	36(3)	First	380(3)	4.4(4)	27(3)	127(3)
$NdMn_{1.9}Ti_{0.1}Si_2$	22	First	374	3.6	15.3	99
$NdMn_{1.8}Ti_{0.2}Si_2$	16	First	365	3.2	13	89
$NdMn_{1.7}Ti_{0.3}Si_2$	14	First	360	3	10	70

Table 3. Structural and magnetic parameters of $NdMn_{1.9}Ti_{0.1}Si_2$ as derived from Rietveld refinements of the neutron diffraction patterns and the BLOKJE program. μ_{total}^{Mn} - the Mn magnetic moment; μ_c^{Mn} - the Mn moment along the c-axis; μ_{ab}^{Mn} - the Mn moment in (001) Mn layers; μ^{Nd} - the Nd moment along the c-axis; the errors for the data at T=3 K are shown as typical examples.

T (K)	3 K	15 K	25 K	35 K	50 K	150 K	200 K	300 K	450 K
a(Å)	4.001(7)	4	3.999	3.998	3.997	4.001	4.003	4.009	4.022
c(Å)	10.523(8)	10.522	10.535	10.536	10.535	10.543	10.548	10.558	10.574
V(Å^3)	168.39(8)	168.38	168.43	168.44	168.42	168.74	169.04	169.73	171.13
$d_{Mn\text{-}Mn}$(Å)	2.8286(9)	2.8285	2.8273	2.8272	2.8271	2.8288	2.8307	2.8351	2.8446
Z_{Si}	0.3793(6)	0.3813	0.3807	0.3812	0.3813	0.3789	0.3786	0.3809	0.381
μ_{total}^{Mn}	1.56(4)	1.54	1.67	1.98	2.1	1.91	1.85	1.53	-
μ_c^{Mn}	1.30(6)	1.26	1.67	1.98	2.1	1.91	1.85	1.53	-
μ_{ab}^{Mn}	0.86(2)	0.89	-	-	-	-	-	-	-
μ^{Nd}	2.56(5)	2.77	-	-	-	-	-	-	-
R_{wp}	5.46	5.87	5.99	6.21	6.59	6.93	7.35	7.75	8.05
R_{exp}	3.23	3.45	3.95	4.67	4.89	5.04	5.25	5.65	5.78

Figures

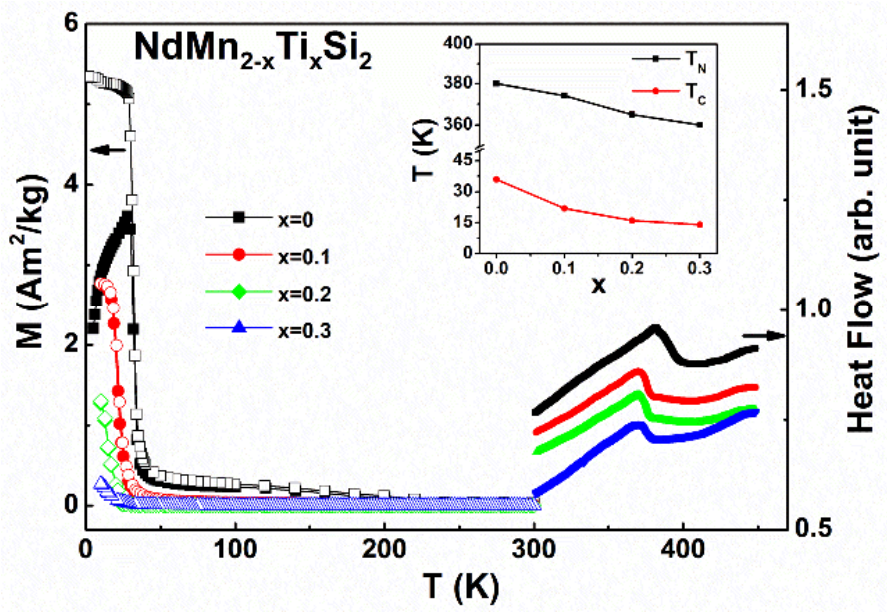

Figure 1. Temperature dependence of magnetization of $NdMn_{2-x}Ti_xSi_2$ compounds (x = 0, 0.1, 0.2, and 0.3) as measured in a field of 0.01 T (left axis; solid symbols for zero field cooling, ZFC, and open symbol for field cooling, FC); and differential scanning calorimetry measurements for the temperature range 300-450 K (right axis; solid symbols). The inset shows the Néel temperatures (T_N) and the Curie temperatures (T_C) for the set of samples.

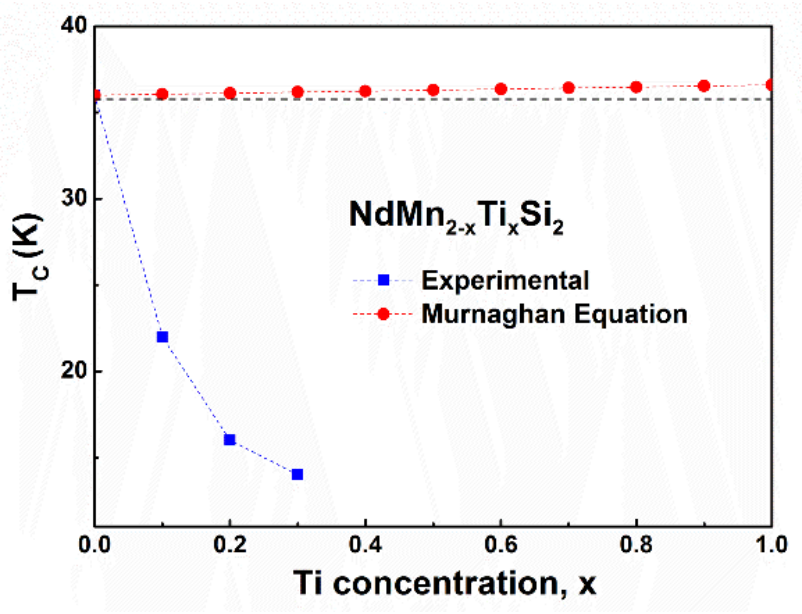

Figure 2. Experimental (squares) and calculated values (circles) of the Curie temperature T_C as a function of Ti concentration for $NdMn_{2-x}Ti_xSi_2$ (x = 0, 0.1, 0.2, 0.3). The T_C values were calculated using the Murnaghan equation and dT_C/dp = -0.6 K/kbar as described in the text. The dashed lines act as a guide to the eye with the horizontal dashed line included to emphasise the slight increase in the calculated T_C values, with increasing Ti concentration.

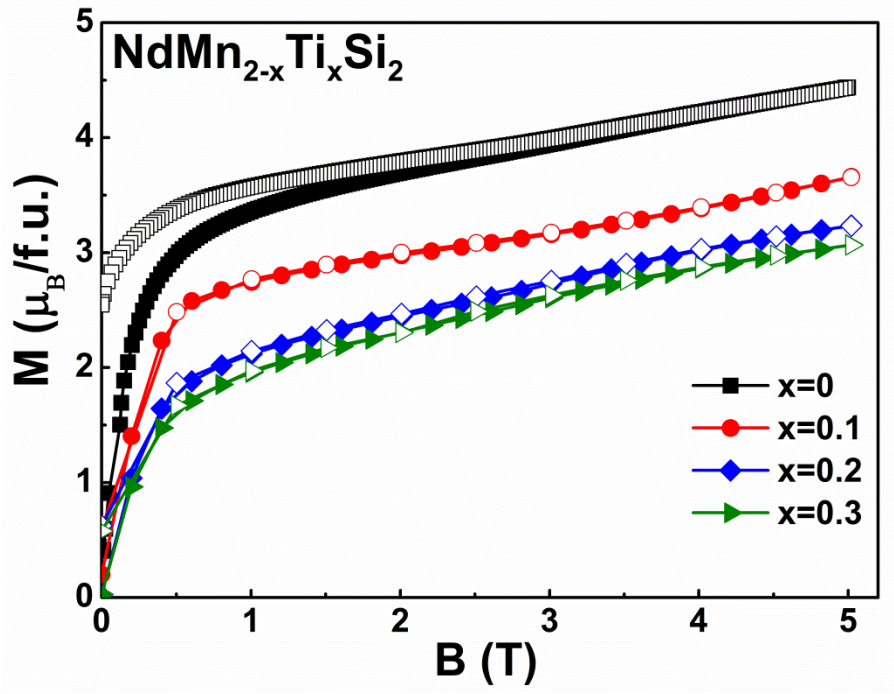

Figure 3. Magnetization curves (B = 0 - 5 T) for $NdMn_{2-x}Ti_xSi_2$ compounds (x = 0, 0.1, 0.2, 0.3) at T = 10 K (closed symbols denote field increasing and open symbols field decreasing).

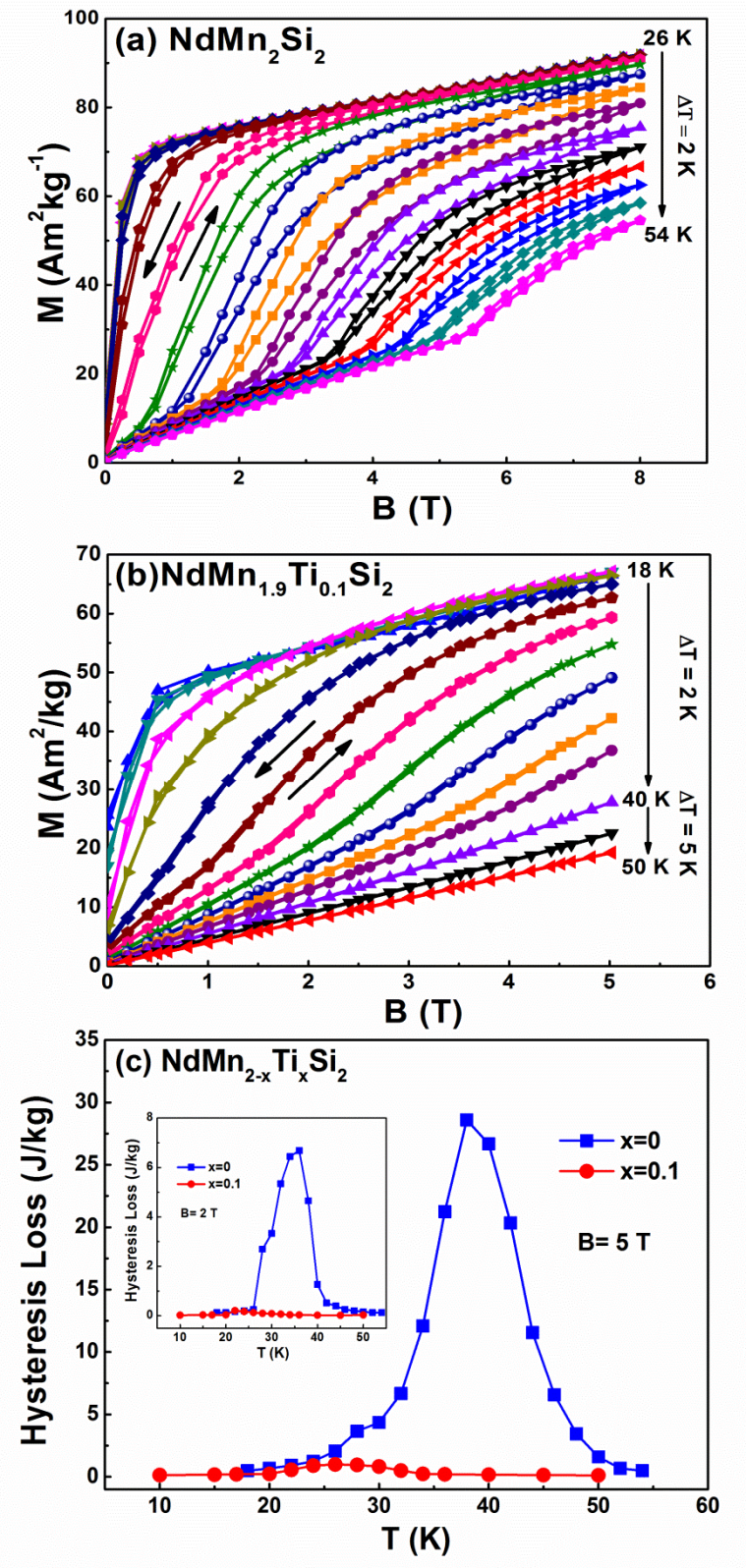

Figure 4. Isothermal magnetization curves in the vicinity of the ferromagnetic ordering temperatures for: (a) $NdMn_2Si_2$ (T_C = 36 K with B = 0 - 8 T) and (b) $NdMn_{1.9}Ti_{0.1}Si_2$ (T_C = 22 K with B = 0 - 5 T) (the arrows indicate the direction of the applied fields during magnetisation measurements, and (c) Comparison of the magnetic hysteresis losses for $NdMn_2Si_2$ and $NdMn_{1.9}Ti_{0.1}Si_2$ for magnetic fields over the ranges B=0-5 T (the results for B=0-2 T are shown in the insert).

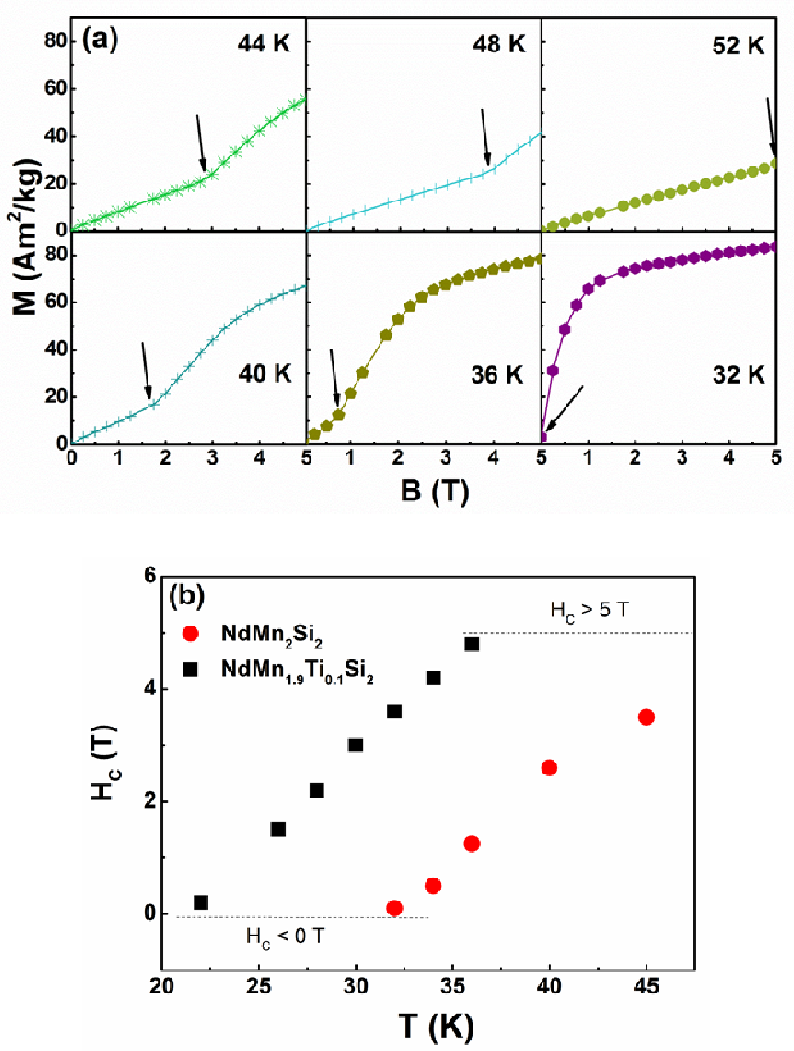

Figure 5. (a) Magnetic field dependence of the magnetization for applied fields in the range 0-5 T at selected temperatures for $NdMn_2Si_2$. H_C corresponds to the field at the onset of the antiferromagnetic to ferromagnetic transition, indicated by arrow; (b) Critical field values, H_C, for $NdMn_2Si_2$ and $NdMn_{1.9}Ti_{0.1}Si_2$ at selected temperatures.

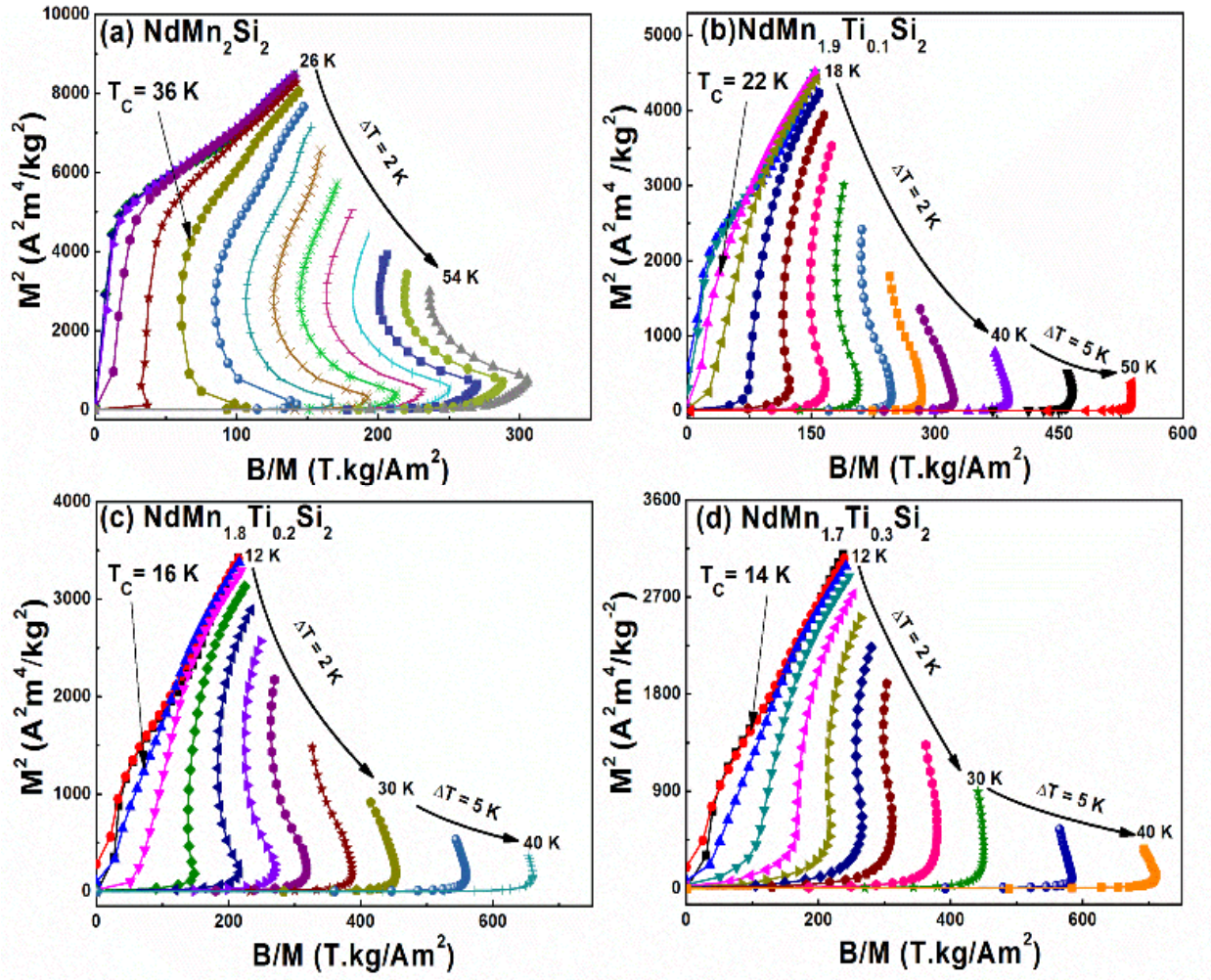

Figure 6. Arrott plots of M^2 versus B/M for the set of $NdMn_{2-x}Ti_xSi_2$ compounds: (a) $NdMn_2Si_2$; (b) $NdMn_{1.9}Ti_{0.1}Si_2$, (c) $NdMn_{1.8}Ti_{0.2}Si_2$, and (d) $NdMn_{1.7}Ti_{0.3}Si_2$.

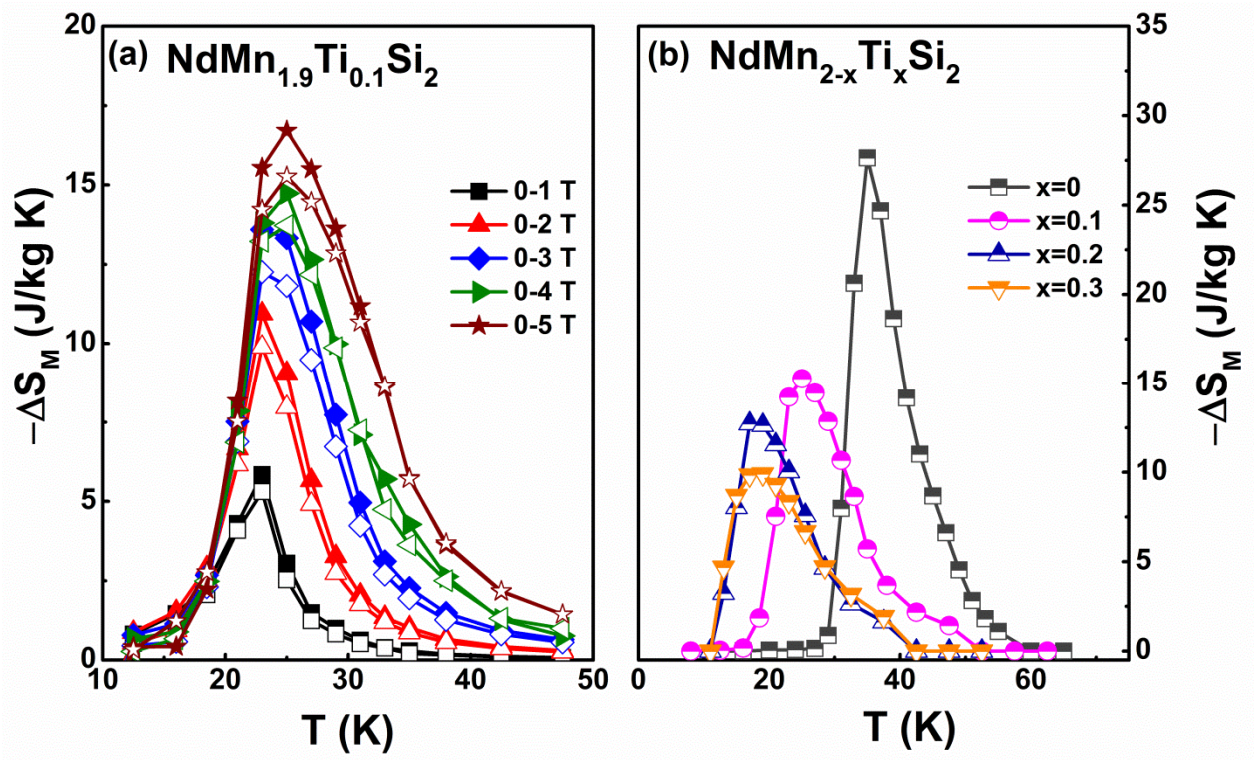

Figure 7. (a) The temperature dependence of the isothermal magnetic entropy change, $-\Delta S_M$, for $NdMn_{0.9}Ti_{0.1}Si_2$ as determined from the magnetization isotherms for ΔB = 0-1 T, ΔB = 0-2 T, ΔB = 0-3 T, ΔB = 0-4 T and ΔB = 0-5 T (closed symbols for increasing fields and open symbols for decreasing fields). (b) The temperature dependence of the isothermal magnetic entropy change, $-\Delta S_M$, for $NdMn_{2-x}Ti_xSi_2$ compounds with x = 0, 0.1, 0.2 and 0.3 as measured from magnetization isotherms (ΔB = 0-5 T from decreasing field curves).

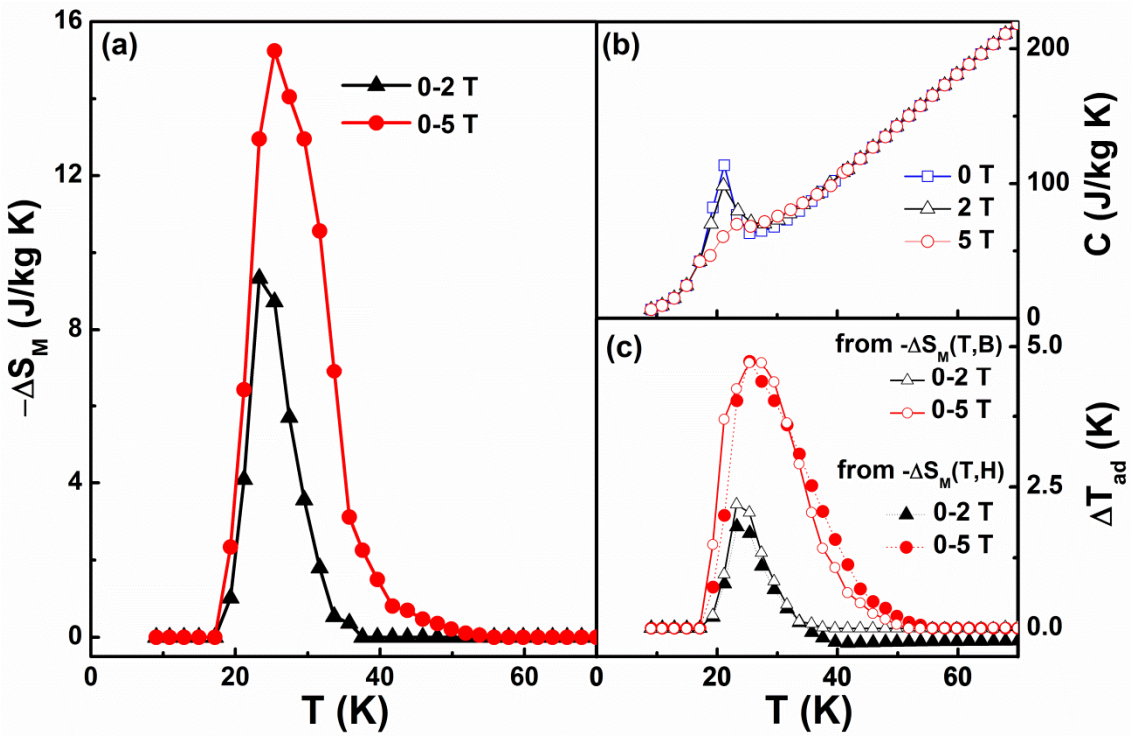

Figure 8. (a) The magnetic entropy change, $-\Delta S_M$, determined from the heat capacity measurements of figure 8(b) for $NdMn_{1.9}Ti_{0.1}Si_2$ (ΔB = 0-2 T, ΔB = 0-5 T). (b) The heat capacity of $NdMn_{1.9}Ti_{0.1}Si_2$ as measured over the temperature range 10-70 K in magnetic fields B = 0 T, 2 T, 5 T. (c) The adiabatic temperature change, ΔT_{ad}, for $NdMn_{1.9}Ti_{0.1}Si_2$ as determined from the heat capacity(open symbol) of figure 8(b) and magnetization (closed symbol) measurements.

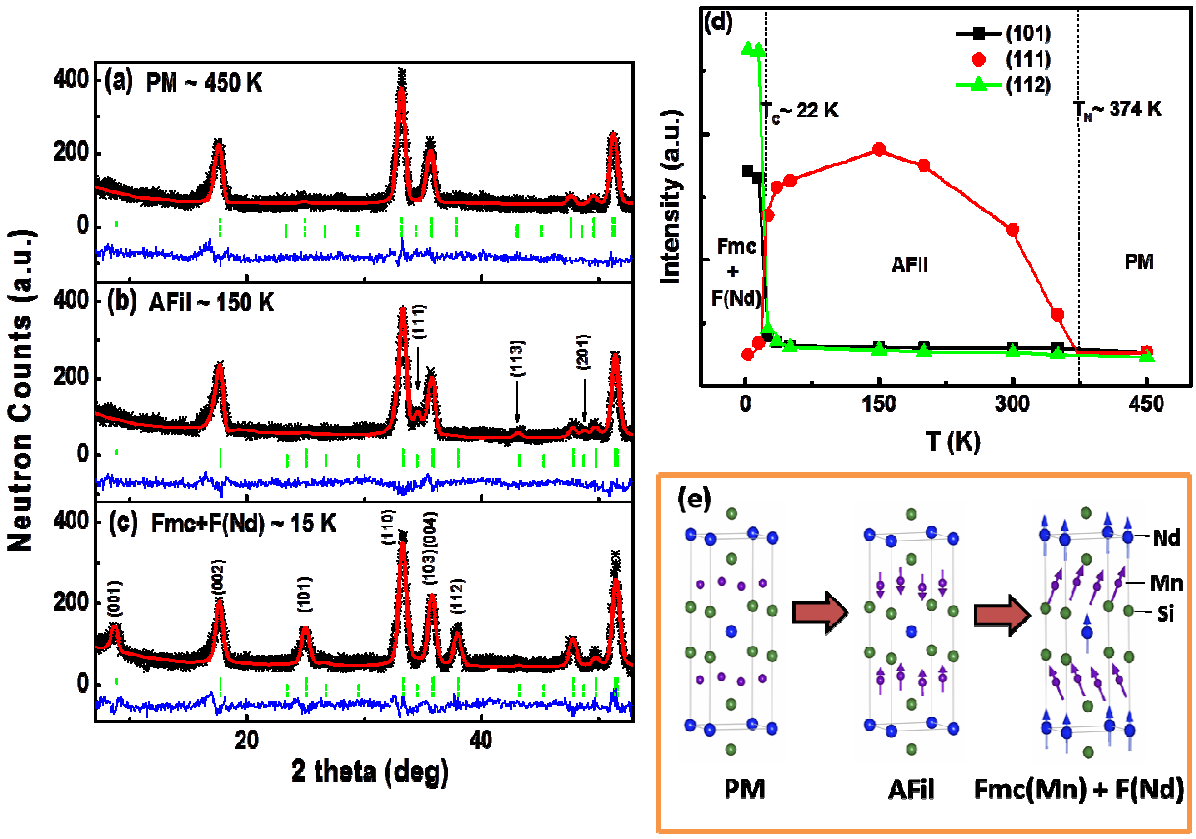

Figure 9. (a), (b), and (c) Neutron diffraction patterns for $NdMn_{1.9}Ti_{0.1}Si_2$ at 450 K, 150 K, and 15 K respectively. The star symbols represent the observed patterns and the red solid lines the refined patterns. The blue lines represent the differences between the observed and refined patterns; the vertical bars indicate the Bragg peak positions for the nuclear (top), Fmc magnetic (middle) and AFil magnetic (bottom) structure respectively. (d) The temperature dependence of the integrated intensities of the (101), (112) and (111) reflections for $NdMn_{1.9}Ti_{0.1}Si_2$ over the temperature range 3-450 K. The T_N ~ 374 K and T_C ~ 22 K transition temperatures that delineate the paramagnetic PM, antiferromagnetic AFil and ferromagnetic Fmc+F(Nd) regions, asre shown by the dashed lines. The lines through the intensity values act as guides to the eye. (e) The structure of $NdMn_{1.9}Ti_{0.1}Si_2$ and the antiferromagnetic AFil and ferromagnetic Fmc+F(Nd) structures.

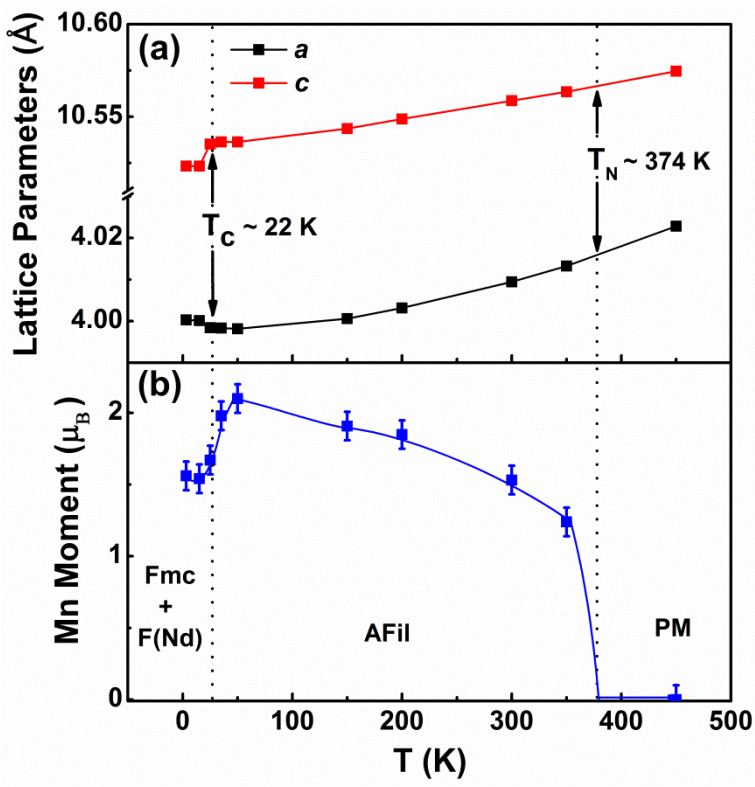

Figure 10. (a) The lattice parameters of $NdMn_{1.9}Ti_{0.1}Si_2$ as a function of temperature and (b) temperature dependence of the Mn magnetic moment (3-450 K). The Néel temperature T_N and Curie temperature T_C are denoted by arrows with the dotted lines delineating the paramagnetic (PM), antiferromagnetic (AFil-type) and ferromagnetic (Fmc+F(Nd)) regions. The line through the moment values act as a guide to the eye.

References

[1] Glanz J 1998 *Science* **279** 2045
[2] Gschneidner Jr K A and Pecharsky V K 2008 *International Journal of Refrigeration* **31** 945
[3] Fujita A and Yako H 2012 *Scripta Materialia* **67** 578
[4] Trung N T, Zhang L, Caron L, Buschow K H J and Bruck E 2010 *Applied Physics Letters* **96** 172504
[5] Liu E, Wang W, Feng L, Zhu W, Li G, Chen J, Zhang H, Wu G, Jiang C, Xu H and de Boer F 2012 *Nat Commun* **3** 873
[6] Pecharsky V K and Gschneidner J K A 1997 *Physical Review Letters* **78** 4494
[7] Yan A, Muller K H, Schultz L and Gutfleisch O 2006 *Journal of Applied Physics* **99** 08K903
[8] Wada H and Tanabe Y 2001 *Applied Physics Letters* **79** 3302
[9] Shen J, Li Y X, Dong Q Y and Sun J R 2009 *Journal of Magnetism and Magnetic Materials* **321** 2336
[10] Szytuła A and Leciejewicz J 1989 in *Chapter 83 Magnetic properties of ternary intermetallic compounds of the RT2X2 type Vol.* ***Volume 12*** Eds.: Karl A. Gschneidner, Jr. and LeRoy E), Elsevier, pp. 133
[11] Emre B, Aksoy S, Posth O, Acet M, Duman E, Lindner J and Elerman Y 2008 *Physical Review B* **78** 144408
[12] Venturini G, Welter R, Ressouche E and Malaman B 1995 *Journal of Magnetism and Magnetic Materials* **150** 197
[13] Venturini G, Welter R, Ressouche E and Malaman B 1995 *Journal of Alloys and Compounds* **224** 262
[14] Samanta T, Das I and Banerjee S 2007 *Applied Physics Letters* **91** 152506
[15] Kumar P, Suresh K G, Nigam A K, Magnus A, Coelho A A and Gama S 2008 *Physical Review B* **77** 224427
[16] J L Wang, S J Campbell, A J Studer, M Avdeev, R Zeng and Dou S X 2009 *Journal of Physics: Condensed Matter* **21** 124217
[17] Wang J L, Campbell S J, Cadogan J M, Studer A J, Zeng R and Dou S X 2011 *Applied Physics Letters* **98** 232509
[18] Wang J L, Campbell S J, Cadogan J M, Studer A J, Zeng R and Dou S X 2011 *Journal of Physics: Conference Series* **303** 012022
[19] Szytuła A and Siek S 1982 *Journal of Magnetism and Magnetic Materials* **27** 49
[20] Fujii H, Okamoto T, Shigeoka T and Iwata N 1985 *Solid State Communications* **53** 715
[21] Fujii H, Isoda M, Okamoto T, Shigeoka T and Iwata N 1986 *Journal of Magnetism and Magnetic Materials* **54–57, Part 3** 1345
[22] Welter R, Venturini G, Fruchart D and Malaman B 1993 *Journal of Alloys and Compounds* **191** 263
[23] Wang Y-g, Yang F, Chen C, Tang N and Wang Q 1997 *Journal of Alloys and Compounds* **257** 19
[24] Kolmakova N P, Sidorenko A A and Levitin R Z 2002 *Low Temperature Physics* **28** 653
[25] Yusuf S M, Halder M, Rajarajan A K, Nigam A K and Banerjee S 2012 *Journal of Applied Physics* **111** 093914
[26] Wang J L, Campbell S J, Studer A J, Avdeev M, Hofmann M, Hoelzel M and Dou S X 2008 *Journal of Applied Physics* **104** 103911
[27] L. B. McCusker, R. B. Von Dreele, D. E. Cox, D. Louër and Scardi P 1999 *Journal of Applied Crystallography* **32** 36
[28] Siek S, Szytuła A and Leciejewicz J 1981 *Solid State Communications* **39** 863
[29] Gelato L 1981 *J. Appl. Crystallogr.* **14** 151
[30] Fukuhara T, Maezawa K, Ohkuni H, Kagayama T and Oomi G 1997 *Physica B: Condensed Matter* **230–232** 198
[31] Di Napoli S, Llois A M, Bihlmayer G and Blügel S 2007 *Physical Review B* **75** 104406
[32] Kawashima T, Kanomata T, Yoshida H and Kaneko T 1990 *Journal of Magnetism and Magnetic Materials* **90–91** 721
[33] Obermyer R, Sankar S G and Rao V U S 1979 *Journal of Applied Physics* **50** 2312

[34] Chen Y-Q, Luo J, Liang J-K, Li J-B and Rao G-H 2009 *Chinese Physics B* **18** 4944
[35] Shamba P, Debnath J C, Zeng R, Wang J L, Campbell S J, Kennedy S J and Dou S X 2011 *Journal of Applied Physics* **109** 07A940
[36] Zeng R, Wang J L, Lu L, Li W X, Campbell S J and Dou S X 2010 *Journal of Alloys and Compounds* **505** L38
[37] Feng-xia H, Bao-gen S, Ji-rong S, Zhao-hua C and Xi-xiang Z 2000 *Journal of Physics: Condensed Matter* **12** L691
[38] Caron L, Ou Z Q, Nguyen T T, Cam Thanh D T, Tegus O and Brück E 2009 *Journal of Magnetism and Magnetic Materials* **321** 3559
[39] Li B, Hu W J, Liu X G, Yang F, Ren W J, Zhao X G and Zhang Z D 2008 *Applied Physics Letters* **92** 242508
[40] Zhang X X, Wang F W and Wen G H 2001 *Journal of Physics: Condensed Matter* **13** L747
[41] Pecharsky V K and Gschneidner J K A 1999 *Journal of Applied Physics* **86** 565
[42] Ekkes B 2005 *Journal of Physics D: Applied Physics* **38** R381
[43] GschneidnerJr K A, Pecharsky V K and Tsokol A O 2005 *Reports on Progress in Physics* **68** 1479
[44] Nikitin S A, Popov Y F, Torchinova R S, Tishin A M and Arkharov I A 1987 *Fizika Tverdogo Tela* **29** 572
[45] Balli M, Rosca M, Fruchart D and Gignoux D 2009 *Journal of Magnetism and Magnetic Materials* **321** 123
[46] Hofmann M, Campbell S J and Edge A V J 2004 *Physical Review B* **69** 174432
[47] Dincer I, Elerman Y, Elmali A, Ehrenberg H and André G 2007 *Journal of Magnetism and Magnetic Materials* **313** 342
[48] Welter R, Venturini G, Ressouche E and Malaman B 1995 *Journal of Alloys and Compounds* **218** 204
[49] Coey J M D 2005 *Solid State Sciences* **7** 660
[50] Chatterji T, Combet J, Frick B and Szyula A 2012 *Journal of Magnetism and Magnetic Materials* **324** 1030
[51] Gschneidner Jr K A, Mudryk Y and Pecharsky V K 2012 *Scripta Materialia* **67** 572
[52] Wang J L, Caron L, Campbell S J, Kennedy S J, Hofmann M, Cheng Z X, Md Din M F, Studer A J, Brück E and Dou S X 2013 *Physical Review Letters* **110** 217211